*29th EPS Conference on Plasma Phys. and Contr. Fusion Montreux, 17-21 June 2002 ECA Vol. **26B**, P-2.120 (2002)*

Evaluations of Optimal Pellet Injection Parameters and Expected Detector Signals for the PCX Diagnostics on LHD

V.Yu. Sergeev[1)], O.A. Bakhareva[1)], B.V. Kuteev[1)], N. Tamura[2)], P.R. Goncharov[2)], K.Khlopenkov[3)], A.V. Krasilnikov[4)], M. Isobe[3)], T. Ozaki[3)], M. Sasao[3)] and S. Sudo[3)]

[1)]State Polytechnical University of St. Petersburg, 195251, Russia, e-mail: sergeev@phtf.stu.neva.ru
[2)]Graduate University for Advanced Studies, Hayama, 240-0193, Japan, e-mail: ntamura@nifs.ac.jp
[3)]National Institute for Fusion Science, Oroshi-cho 322-6, Toki 509-5292, e-mail: sudo@nifs.ac.jp
[4)]TRINITI, Troitsk, Moscow region, 142092, Russia, e-mail: anatoli@triniti.ru

Introduction. Understanding the fast particle behavior in high-temperature magnetically confined stellarator plasmas becomes more and more important while plasma parameters grow up to the reactor-like level. A perspective active method of fast ion analysis is the Pellet Charge eXchange (PCX) diagnostics [1], which is based on ion neutralization in a pellet ablation cloud. This diagnostics has been successfully applied on TFTR for studies of fusion alpha particles and tritons [2-3] and tritium minority ions [4]. An application of the PCX diagnostics for the W7-X stellarator plasmas has been proposed in Ref. [5], considering a Li pellet cloud as a target for CX of fast ICRF-driven protons, and the Neutral Particle Analyzer (NPA) [4] as a spectrometer of escaping neutrals. In this work, simulations of signals for the PCX diagnostics on LHD, which uses lithium and polystyrene $(C_8H_8)_n$ pellets, are carried out. Along with the NPA, the Natural Diamond Detector (NDD) [6] is considered as an energy spectrometer of neutrals. Pellet ablation rates and cloud sizes in different ICRF and NBI -heated LHD regimes were simulated in order to estimate optimal pellet size and velocity as well as the detector count rate.

Pellet ablation simulations. Li and $(C_8H_8)_n$ pellet ablation rate has been simulated using the Neutral Gas and Electrostatic Shielding Model (NGESM) [5], which allows us to take into account the effect of fast particles on ablation. The heat flows of fast ICRF-driven protons and fast NBI ions were evaluated using the distribution functions obtained in the classical slowing-down approach [7,8], but for the ICRF-driven protons the characteristic slowing-down time was restricted by the energy confinement time found from the LHD scaling [10,11]. The following model parameters and assumptions have been used for the ablation simulations: 1) the electron and ion temperature profiles $T_e, T_i = T_{e0}, T_{i0} \times (1 - \rho^2)^2$ versus the effective minor radius ρ, the electron density profile $n_e = n_{e0} \times (1 - \rho^8)^2$; 2) two regimes with the following central values: $n_{e0} = 1.5 \cdot 10^{19}$ m^{-3}, $T_{e0} = 2$ keV, $T_{i0} = 0.8$ keV for Regime 1 and

$n_{e0} = 0.7 \cdot 10^{19}$ m^{-3}, $T_{e0} = 4$ keV, $T_{i0} = 2$ keV for Regime 2; 3) the minority H^+ ions content $\alpha = n_H/n_{He} = 0.01$ or 0.05; 4) the total ICRH power absorbed by the H^+ minority P_{ICRH} - 1 MW and 3 MW; 5) the deposition profile of the ICRH power - Type A and Type B, which are shown in Fig. 1 by the dotted and the solid lines correspondingly; 6) the neutral beam energy 150 keV, the port-through NBI heating power 4 MW, 20% of which is evaluated to be deposited into ions; 7) the NBI power deposition profile is proportional to n_e. The pellet size r_{p0} was chosen as that providing the electron density perturbation after injection equal to the initial electron content in the plasma. The «optimal» pellet velocity v_p^{opt} was found from the condition of pellet reaching the plasma center. The pellet sizes and velocities in different LHD regimes are given in Tables 1 and 2 for Li and $(C_8H_8)_n$ pellets correspondingly.

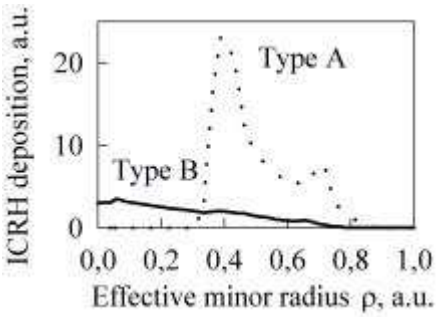

Fig. 1. The model ICRH power deposition profiles in LHD.

Table 1 v_p^{opt} (km/s) for Li		Regime 1 (r_{p0} = 0.8 mm)		Regime 2 (r_{p0} = 0.62)	
		$\alpha = 0.05$	$\alpha = 0.2$	$\alpha = 0.05$	$\alpha = 0.2$
P_{ICRH} = 1 MW	Type A	0.23	0.22	0.70	0.70
	Type B	0.24	0.22	0.70	0.70
P_{ICRH} = 3 MW	Type A	0.35	0.27	0.90	0.75
	Type B	0.55	0.32	1.10	0.80

Table 2 v_p^{opt} (km/s) for $(C_8H_8)_n$		Regime 1 (r_{p0} = 0.59 mm)		Regime 2 (r_{p0}=0.46 mm)	
		$\alpha = 0.05$	$\alpha = 0.2$	$\alpha = 0.05$	$\alpha = 0.2$
P_{ICRH} = 1 MW	Type A	0.65	0.65	2.10	2.10
	Type B	0.66	0.65	2.10	2.10
P_{ICRH} = 3 MW	Type A	0.90	0.70	2.50	2.20
	Type B	1.25	0.80	2.70	2.20

From Tables 1,2 it follows that 1) the v_p^{opt} values are 2-3 times larger in the Regime 2 compared to the Regime 1; 2) the v_p^{opt} values for Type A are 1.0-1.6 times greater than for Type B, 3) ablation is stronger and v_p^{opt} is 1-2.3 times higher for regimes with greater values of P_{ICRH} and a smaller minority fraction α. An additional experimental investigation of pellet ablation in ICRF-heated LHD regimes is desirable.

Both the fast CX neutrals flux emitted from the pellet cloud and the PCX detector signal depend on the transverse cloud size. Following to Ref. [9], two estimations of the transverse cloud size have been made. The radius of the cloud plateau r_{pl} was estimated from the energy balance between the electron heat flux flowing onto the cloud from the bulk plasma and the energy required to evaporate, dissociate (if necessary), heat accelerate and ionize the evapo-

rated material. The "exponential wings" scale was also estimated as the ionization length of the ablated neutrals to the first charge state (r_{ion}). Thus, for Li pellets we obtained r_{pl}^{Li} ~ 0.5-1.5 mm, r_{ion}^{Li} ~ 1-3 cm, while for $(C_8H_8)_n$ pellets $r_{pl}^{C,H}$ ~ 1-2 mm, $r_{ion}^{C,H}$ ~ 0.5-5 cm. For both cases, the size of the cloud plateau is small compared to the transverse decay length. This means that the slowly decaying "exponential wings" length should give a contribution to the fast particles CX. For simplicity, the cloud plateau size values were used for the PCX signals simulation. Such simplification might yield underestimated PCX signals.

Estimation of the PCX signals

The count rate of both the NPA and NDD detector depends on 1) the proton energy distribution function, 2) neutralization properties of the cloud, 3) detector parameters.

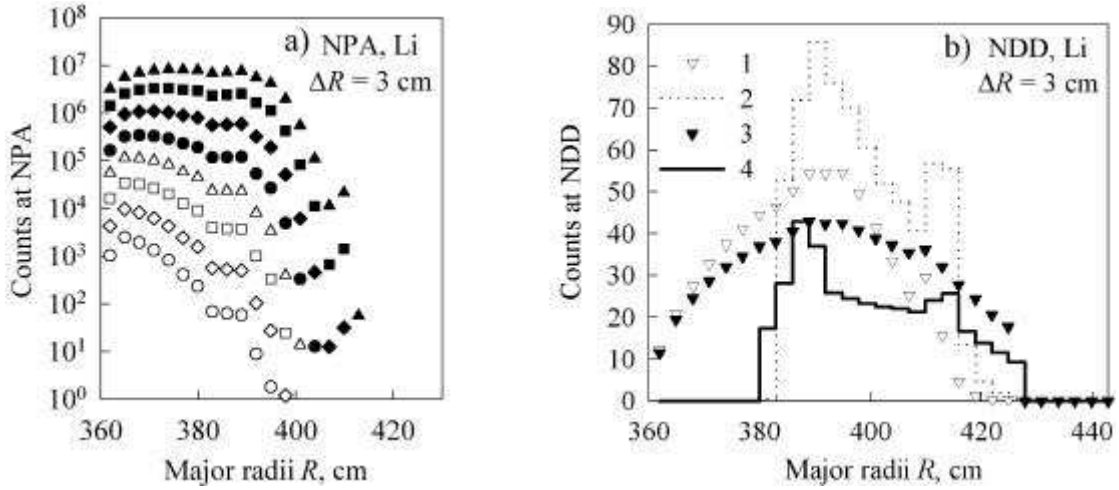

Fig. 2. The simulated counts profiles along the pellet trajectory: **a)** at the NPA for the Regime 1, ICRH Type B, P_{ICRH} =3 MW, α = 0.05. The symbols from upper to lower curve correspond to the neutrals energies E (and energy resolutions $\Delta E/E$) 266 keV (0.113), 322 keV (0.094), 404 keV (0.085), 498 keV (0.074), 608 keV (0.067), 727 keV (0.061), 857 keV (0.058), 1 MeV (0.056). **b)** at the NDD for the regimes 1) Regime 1, Type B, P_{ICRH} = 3 MW, α = 0.05, S_c = $8.5 \cdot 10^{-8}$ cm^2, 2) Regime 1, Type A, P_{ICRH} = 3 MW, α = 0.05, S_c = $7.9 \cdot 10^{-8}$ cm^2, 3) Regime 2, Type B, P_{ICRH} = 1 MW, α = 0.2, S_c = $1.6 \cdot 10^{-6}$ cm^2, 4) Regime 2, Type A, P_{ICRH} = 1 MW, α = 0.2, S_c = $9.4 \cdot 10^{-7}$ cm^2. The magnetic axis is at R=360 cm, separatrix is at R=446 cm.

In the current simulations, eq. (4) from Ref. [5] was used for the count rate calculation. The H^+ distribution function was taken from Ref. [7]. The fraction of neutralized protons was calculated using the CX cross-sections of H^+ and H^0 in a 100% Li^+ and in a (25% C^{1+}, 25% C^{2+}, 50% H^0) clouds. For details and for the detector parameters see Ref. [5, 6]. For Li clouds, the count rate profiles over the time intervals $\Delta t = \Delta R / v_p^{opt}$ (here the spatial resolution ΔR = 3cm and v_p^{opt} is given in Table 1) are shown in Figs. 2a and 2b for the NPA and NDD detectors correspondingly. The signal in Fig. 2a might be well detectable by the NPA. In the case of $(C_8H_8)_n$ cloud, the NPA signal is an order of magnitude greater. The profiles in Fig. 2b were obtained with the restriction on the area of the NDD collimating aperture S_c, which

should provide the count rate below the maximum acceptable value at a 3 cm desired spatial resolution. The values in Fig. 2b are essentially less than the count rate necessary for the energy spectrum with good statistics (1000-2000 counts). Therefore, achievement of a good statistics over the whole energy range together with acceptable spatial resolution seems to be a technical problem for the NDD operating with analog spectroscopy electronics at count rate up to 10^6 cps.

Summary. The ablation behavior of lithium and polystyrene pellets has been simulated in various LHD He plasma regimes with ICRF driven H^+ minority. The simulations showed that for pellet penetration to the plasma core it is preferable to inject pellets in regimes with higher plasma density and lower plasma temperature, with lower ICRH power, with a larger minority fraction, and when the ICRH power is deposited closer to plasma periphery. Li pellets of 1.2-1.6 mm in size and with 0.2-1.1 km/s velocities can provide a core pellet penetration in the regimes simulated. For polystyrene pellets of 0.9-1.2 mm size (with the same electron content), higher 0.65-2.7 km/s velocities are required for the core penetration. Estimations of the PCX neutrals energy spectra for LHD made for two types of detectors NDD and NPA show that for both Li and $(C_8H_8)_n$ pellets, the estimated number of the incident fast CX neutrals can be well detected by the E||B NPA with spatial resolution of about 3 cm in those regimes, where a visible effect of the ICRF driven protons on pellet ablation is expected. For the NDD at count rate up to 10^6 cps, a lack of statistics over the whole energy range is expected at an acceptable (3 cm) spatial resolution.

References

[1] R.K. Fisher, *et al.* Fusion Technol. **13** (1988) 536.

[2] S.S. Medley, *et al.* Rev. Sci. Instrum. **67** (1996) 3122.

[3] J.M. McChesney, *et al.* Rev. Sci. Instrum. **66** (1995) 348.

[4] M.P. Petrov, *et al.* Phys. of Plasm. **6** (1999) 2430.

[5] V.Yu. Sergeev *et al*. IPP Report 10/20, January 2002.

[6] A.V. Krasilnikov *et.al.* Nucl.Fusion, **39** (1999) 1111. See also P.R. Goncharov *et al.* in this conference.

[7] T.H. Stix, Nuclear Fusion **15** (1975) 737.

[8] D.E. Post, *et al.* Journal of Fusion Energy, Vol. 1,No. 2, 1981.

[9] B.V. Kuteev, *et al.* Journal of Technical Phys., Vol. 72, No. 8, 2002.

[10] M. Fujiwara, *et al.* Plasma Physics and Controlled Fusion **41** (1999) B157-B166.

[11] H. Yamada, *et al.* Plasma Physics and Controlled Fusion **43** (2001) A55-A71.